

# Cdc42 and Actin Control Polarized Expression of TI-VAMP Vesicles to Neuronal Growth Cones and Their Fusion with the Plasma Membrane<sup>□</sup>

Philipp Alberts,<sup>\*†‡</sup> Rachel Rudge,<sup>\*†</sup> Theano Irinopoulou,<sup>§</sup> Lydia Danglot,<sup>\*†</sup>  
Cécile Gauthier-Rouvière,<sup>||</sup> and Thierry Galli<sup>\*†</sup>

<sup>\*</sup>Membrane Traffic in Neuronal and Epithelial Morphogenesis, Institut National de la Santé et de la Recherche Médicale Avenir Team, 75005 Paris, France; <sup>†</sup>Institut Jacques Monod, Unité Mixte de Recherche 7592 Centre National de la Recherche Scientifique, Universities Paris 6 and 7, 75005 Paris, France; <sup>§</sup>Institut National de la Santé et de la Recherche Médicale U536, Institut du Fer-à-Moulin, 75005 Paris, France; and <sup>||</sup>“Rho GTPases, Adhesion and Skeletal Muscle,” Centre de Recherches de Biochimie Macromoléculaire-Centre National de la Recherche Scientifique Formation de Recherche en Evolution 2593, 34293 Montpellier, France

Submitted July 18, 2005; Revised December 5, 2005; Accepted December 20, 2005  
Monitoring Editor: Jennifer Lippincott-Schwartz

**Tetanus neurotoxin-insensitive vesicle-associated membrane protein (TI-VAMP)-mediated fusion of intracellular vesicles with the plasma membrane is crucial for neurite outgrowth, a pathway not requiring synaptobrevin-dependent exocytosis. Yet, it is not known how the TI-VAMP membrane trafficking pathway is regulated or how it is coordinated with cytoskeletal dynamics within the growth cone that guide neurite outgrowth. Here, we demonstrate that TI-VAMP, but not synaptobrevin 2, concentrates in the peripheral, F-actin-rich region of the growth cones of hippocampal neurons in primary culture. Its accumulation correlates with and depends upon the presence of F-actin. Moreover, acute stimulation of actin remodeling by homophilic activation of the adhesion molecule L1 induces a site-directed, actin-dependent recruitment of the TI-VAMP compartment. Expression of a dominant-positive mutant of Cdc42, a key regulator of cell polarity, stimulates formation of F-actin- and TI-VAMP-rich filopodia outside the growth cone. Furthermore, we report that Cdc42 activates exocytosis of pHluorin tagged TI-VAMP in an actin-dependent manner. Collectively, our data suggest that Cdc42 and regulated assembly of the F-actin network control the accumulation and exocytosis of TI-VAMP-containing membrane vesicles in growth cones to coordinate membrane trafficking and actin remodeling during neurite outgrowth.**

## INTRODUCTION

One of the most striking features of neurons is their extremely elongate form, with their axons and dendrites extending frequently over tens of centimeters. Axons and dendrites elongate through specialized, highly motile growth cones. Leading the movement at the tips of the developing neurites, the growth cones extend by fusing membrane vesicles with their plasma membrane and by the constant growth and reorganization of the cytoskeleton below this plasma membrane that pushes the leading edge forward. Although the role of cytoskeletal dynamics in the navigation of growth cones is well established (Song and Poo, 2001; da Silva and Dotti, 2002), no link has yet been found between the cytoskeleton and the membrane trafficking machinery that delivers membrane vesicles for growth.

Soluble *N*-ethylmaleimide-sensitive factor attachment protein receptors (SNAREs) constitute the core machinery for membrane fusion and are involved in all of the fusion events along the biosynthetic and endocytic pathways (for review, see Rothman, 2002). The membrane fusion mechanism involved in neurite outgrowth differs from the “classical” synaptic core machinery inasmuch as it is unaffected by treatment with tetanus neurotoxin (TeNT), which cleaves the classical synaptic vesicle SNARE synaptobrevin 2 (Syb2) and so blocks neurotransmitter release (Osen-Sand *et al.*, 1996; Grosse *et al.*, 1999). Accordingly, the brains of Syb2 null mice develop normally up to birth (Schoch *et al.*, 2001). In contrast, a specific membrane fusion machinery may be involved in neuronal development because a mutant of the exocyst component Sec5 shows impaired neurite outgrowth but normal release of neurotransmitter in *Drosophila melanogaster* (Murthy *et al.*, 2003). We have shown that a TeNT-insensitive vesicle-associated membrane protein (TI-VAMP; also called VAMP-7), which is also a member of a subfamily of vesicular SNAREs (Filippini *et al.*, 2001; Rossi *et al.*, 2004), plays a major role in neurite outgrowth (Martinez-Arca *et al.*, 2000, 2001; Alberts *et al.*, 2003). However, the precise mechanism by which TI-VAMP-mediated fusion leads to growth and how it is regulated are not known.

In this article, we set out to test the possible coordination of TI-VAMP-mediated trafficking with actin in neuronal

This article was published online ahead of print in *MBC in Press* (<http://www.molbiolcell.org/cgi/doi/10.1091/mbc.E05-07-0643>) on December 28, 2005.

<sup>□</sup> The online version of this article contains supplemental material at *MBC Online* (<http://www.molbiolcell.org>).

<sup>†</sup> Present address: Department of Cell Biology, Yale University School of Medicine, New Haven, CT 06520.

Address correspondence to: Thierry Galli ([thierry@tgalli.net](mailto:thierry@tgalli.net)).

growth cones as a way to integrate membrane traffic and cytoskeleton dynamics in neurite elongation and polarization.

## MATERIALS AND METHODS

### Antibodies and Fluorescent Reagents

Mouse monoclonal antibody (mAb) to TI-VAMP (CI 158.2) was described previously (Muzerelle *et al.*, 2003). The polyclonal anti-green fluorescent protein (GFP) antibody we used was described previously (Martinez-Arca *et al.*, 2001). Mouse mAb against Syb2 (clone 69.1) was a generous gift from R. Jahn (Max Planck Institute, Goettingen, Germany). Mouse monoclonal antibodies against EEA1 and CD63 were from BD Biosciences (Franklin Lakes, NJ) and from Ancell (Bayport, MN), respectively. Polyclonal anti-red fluorescent protein (RFP) antibody (Ab3216) was from Chemicon International (Temecula, CA). Affinity-purified Cy3- and Cy5-coupled goat anti-rabbit and anti-mouse immunoglobulins were from Jackson ImmunoResearch Laboratories (West Grove, PA). Alexa 488-coupled goat anti-rabbit and anti-mouse immunoglobulins and phalloidin coupled to Alexa 564 or 488 were from Molecular Probes (Carlsbad, CA). Fluorescent cholera toxin was a generous gift from L. Johannes (Institut Curie, Paris, France).

### Plasmids

TI-VAMP-ecliptic pHLuorin (TIVAMP-epHL) was described previously (Martinez-Arca *et al.*, 2000). The mutations (F64L and S65T) required to obtain the super ecliptic variant (Sankaranarayanan *et al.*, 2000) were obtained by site-directed mutagenesis in TIVAMP-epHL. Chimeras between red fluorescent protein (mRFP) and Rho GTPases were obtained by inserting a *Nhe1*/*BspE1* fragment from the mRFP1 (a kind gift from R. Tsien, University of California, San Diego, La Jolla, CA) into pEGFP-RhoAL63, pEGFP-Rac1V12 or pEGFP-Cdc42V12 (Gauthier-Rouviere *et al.*, 1998).

### Cell Culture and Transfection

Cos7 cells were maintained in DMEM supplemented with 10% fetal calf serum. Transfection of Cos7 cells was performed using LipofectAMINE, 2000 according to the manufacturer's instructions. Hippocampal and cortical neurons were prepared from E18 rat brain and cultured as described previously (Chang and De Camilli, 2001). Transfection of cortical neurons was performed using the Amaxa Nucleofector (Amaxa, Köln, Germany) according to the manufacturer's recommendations for transfection of primary neurons.

### Qualitative and Quantitative Immunocytochemistry

Cells in culture were fixed with 4% paraformaldehyde/4% sucrose and processed for immunofluorescence microscopy as described previously (Coco *et al.*, 1999). Confocal laser-scanning microscopy was performed using a SP2 confocal microscope (Leica Microsystems, Mannheim, Germany). Images were assembled using Adobe Photoshop (Adobe Systems, San Jose, CA).

For comparing TI-VAMP- or Syb2-expression with F-actin content in growth cones, cells were double-labeled with monoclonal antibodies to TI-VAMP or Syb2 and Alexa564-coupled phalloidin. Images were acquired by confocal microscopy based on the actin staining and therefore blind for TI-VAMP- or Syb2-associated immunoreactivity. The fluorescence intensity of single confocal planes within growth cones was analyzed using the region measurement function of the MetaMorph software (Universal Imaging, Evry France) and a regression analysis was performed to statistically evaluate differences. For evaluation of TIV-, Syb2-, and actin fluorescence intensity in growth cones expressing RFP or Cdc42-RFP, images were acquired from triple-labeled cells (phalloidin A488, RFP, and anti-mouse Cy5) based on RFP signal, i.e., blind for the associated TI-VAMP or actin signal, and analysis was performed as described above. Differences were evaluated statistically with the Mann-Whitney nonparametric test.

### Bead-Cell Adhesion Assay

Purification of L1Fc, production of L1-coated beads, and incubation of hippocampal neurons with L1-coated beads was performed as described in Alberts *et al.* (2003).

### Imaging and Quantification of the Exocytosis of TIV-pHL

TIV-pHL-expressing cells were placed in DMEM without riboflavin in a Ludin Chamber type 1 (LIS, Reinach, Switzerland), and the microscope temperature was controlled using a Cube & Box control system (LIS, Reinach, Switzerland). Movies were acquired on a Leica DM IRBE inverted microscope, under mercury lamp illumination with filters (GFP, excitation  $475 \pm 20$  nm; RFP, excitation  $525 \pm 45$  nm) piloted by a Lambda 10-2 filter wheel (AutoMate Scientific, San Francisco, CA), and acquired with a Cascade amplified camera (Photometrics/Roper Scientific, Evry, France). Images were acquired every 2 s with exposure times between 400 and 600 ms using MetaMorph and treated using the haze removal filtering. Quantification of the number of events was obtained by manual inspection of the movies frame

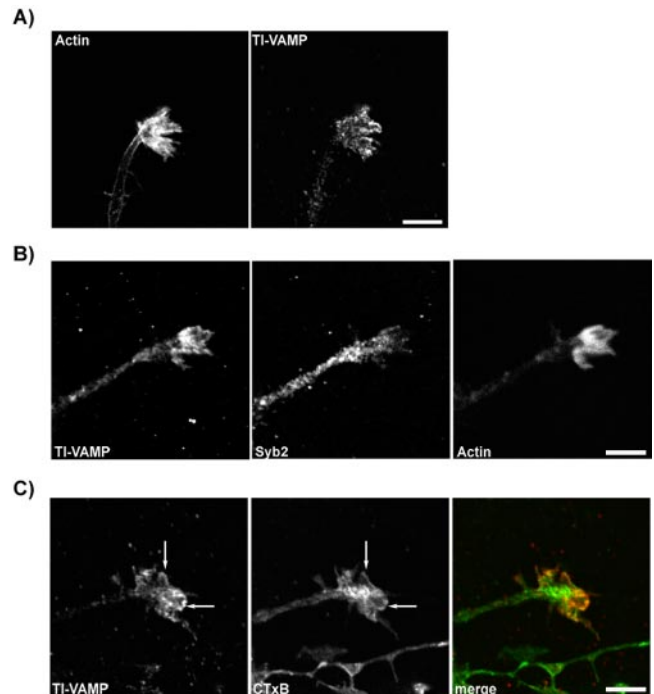


**Figure 1.** Accumulation of TI-VAMP in the F-actin-rich region of axonal growth cones. (A) Cultured hippocampal neurons grown (3 days *in vitro* [div]) were costained for filamentous actin (left) and for TI-VAMP (right) and analyzed by confocal microscopy. Bar, 4  $\mu$ m. (B) A high-magnification confocal image of an axonal growth cone triple-labeled for TI-VAMP (left), Syb2 (middle), and F-actin (right). Bar, 4  $\mu$ m. (C) Living hippocampal neurons were labeled with fluorescent CTxB subunit to stain the plasma membrane (middle and green in merge). Cells were washed, fixed and costained with a mAb against TI-VAMP (left, red in merge). The TI-VAMP signal partially coincides with the plasma membrane staining by CTxB marked by arrows, yellow in merge. Bar, 4  $\mu$ m.

by frame. Fifteen TIV-pHL-expressing cells were analyzed for each experimental condition.

## RESULTS

We analyzed the localization of TI-VAMP in hippocampal neurons in culture by immunofluorescence microscopy and noticed striking accumulation of TI-VAMP in axonal growth cones. Moreover TI-VAMP localizes exclusively to areas that also stained intensely with fluorescent phalloidin, which binds to filamentous (F)-actin (Figure 1A), indicating that TI-VAMP localization is restricted to the so-called actin-rich peripheral domain of axonal growth cones (Suter *et al.*, 1998). This localization of TI-VAMP to the F-actin-rich region of growth cones was specific because, in agreement with our previous findings (Coco *et al.*, 1999), Syb2 was largely excluded from the growth cone periphery (Figure 1B). The immunofluorescent staining of TI-VAMP in actin-rich growth cones outlined the periphery of the growth cone, suggesting that some of the protein was associated with the plasma membrane. To confirm this conclusion, we labeled the plasma membrane of living neurons with a fluorescently labeled B subunit of cholera toxin (CtxB), which binds to GM1 (Guirland *et al.*, 2004), and costained for TI-VAMP after fixation and permeabilization. As shown in Figure 1C, TI-VAMP (green) and CtxB (red) colocalized in the periphery of the growth cone (indicated by arrows)

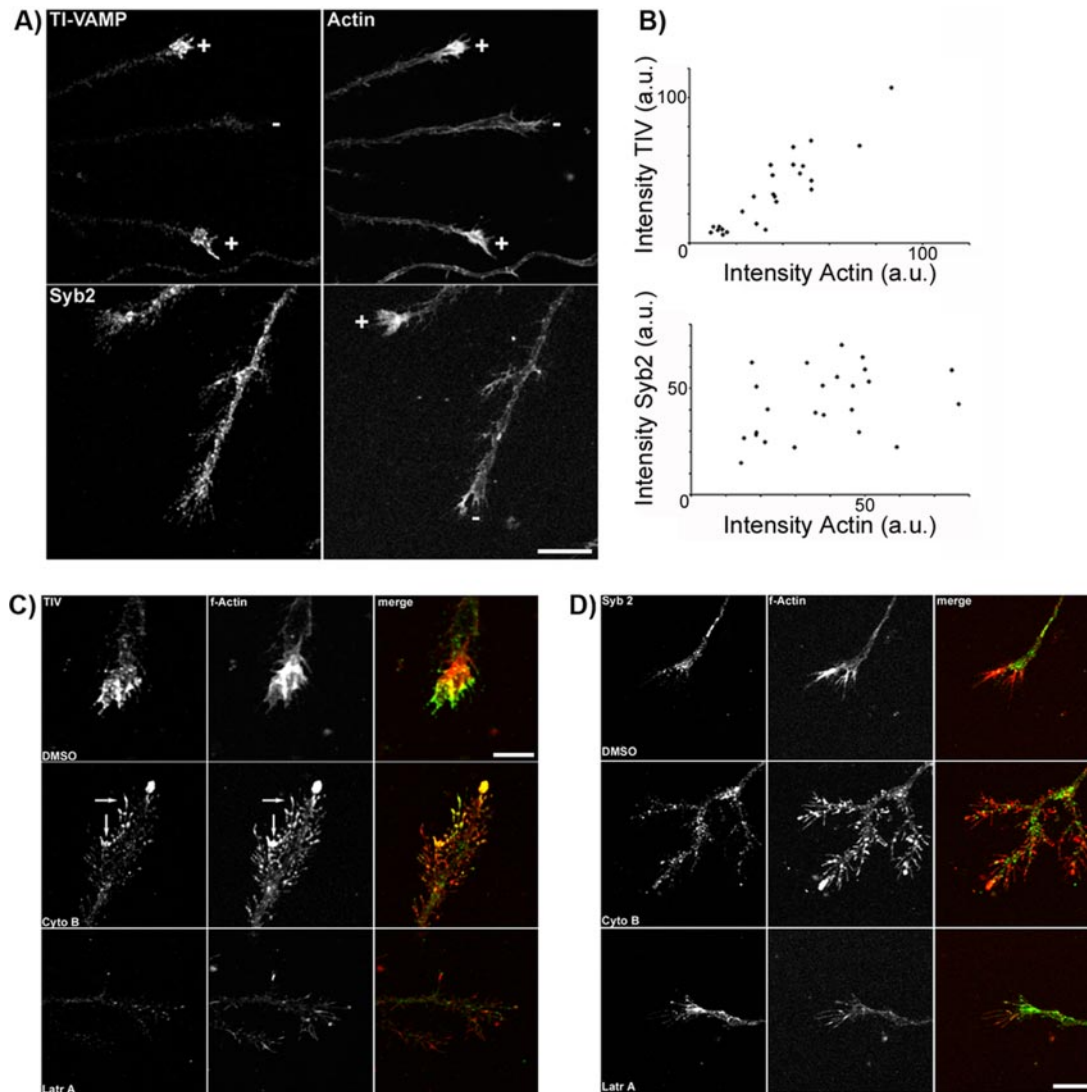


**Figure 2.** TI-VAMP localization in growth cones correlates with and depends upon actin dynamics. (A) Hippocampal neurons 3 div were costained for F-actin and TI-VAMP or Syb2. Labeling intensity was analyzed by confocal microscopy. Top, high labeling intensity of TI-VAMP coincides with high labeling intensity of F-actin (+), and low labeling intensity of TI-VAMP coincides with low labeling intensity of F-actin (-). Syb2 staining does not vary with the intensity of F-actin staining (bottom). Bar, 10  $\mu\text{m}$ . (B) Confocal images of hippocampal neurons stained for TI-VAMP or Syb2 were taken blind based on costaining for F-actin (24 images each). Labeling intensity of each marker in the entire growth cone was quantified and F-actin staining was plotted versus the labeling intensity of associated TI-VAMP (top) or Syb2 (bottom). Whereas TI-VAMP and F-actin labeling intensities are highly correlated ( $Y = -6.771 + 1.185 \cdot X$ ;  $R^2 = 0.818$ ;  $p < 0.0001$ ), the distribution of Syb2- and F-actin-labeling intensities seems random ( $Y = 31.269 + 0.312 \cdot X$ ;  $R^2 = 0.123$ ;  $p = 0.093$ ). (C) Hippocampal neurons (3 div) were treated for 30 min with 5  $\mu\text{M}$  DMSO, 5  $\mu\text{M}$  cytochalasin B (Cyto B), or 2.5  $\mu\text{M}$  latrunculin A (Latr A). Cells were analyzed by confocal microscopy for expression of TI-VAMP (left) and F-actin (right). Treatment with cytochalasin B leads to a redistribution of both F-actin and TI-VAMP to highly fluorescent foci (indicated by arrows). Latrunculin A treatment disrupts the actin cytoskeleton and results in diffuse TI-VAMP staining. (D) Hippocampal neurons grown and treated as in C were analyzed by confocal microscopy for expression of Syb2 (left) and F-actin (right). The distribution of Syb2 seems unaffected by the treatments. Bars, 8  $\mu\text{m}$ .

in regions that are yellow in the merge, confirming the plasma membrane location of TI-VAMP and suggesting that TI-VAMP-mediated vesicle fusion with the plasma membrane might occur at the leading edge of growth cones.

We also noticed that the level of TI-VAMP staining in different growth cones was heterogeneous. Some growth cones were strongly labeled, whereas others were virtually devoid of TI-VAMP staining (Figure 2A, top). Because the actin cytoskeleton in growth cones is known to be highly dynamic (Suter *et al.*, 1998; Song and Poo, 2001), we hypothesized that variations in TI-VAMP staining intensity might

be related to the assembly state of the actin cytoskeleton. As shown in Figure 2A, intense labeling of F-actin in growth cones coincided with intense labeling of TI-VAMP (top, marked with +), whereas growth cones that stained little for F-actin also had little labeling for TI-VAMP (top, marked with -). By contrast, the F-actin content did not correlate with Syb2 labeling intensity in growth cones (Figure 2A, bottom).

To validate these observations, we quantified the F-actin labeling intensity and compared it with the TI-VAMP or Syb2 labeling intensity in a number of growth cones (Figure

2B). Whereas the F-actin intensity correlated closely with TI-VAMP labeling ( $R^2 = 0.818$ ; Figure 2B), we observed no correlation between F-actin and Syb2 labeling intensity in growth cones ( $R^2 = 0.123$ ; Figure 2B). Thus, TI-VAMP expression in growth cones is positively correlated with the regulated assembly of F-actin.

We went on to test whether F-actin formation might play a role in the accumulation of TI-VAMP in growth cones by treating neurons with low concentrations of F-actin-disrupting drugs. As shown in Figure 2C, treatment of hippocampal neurons with cytochalasin B for short times led to a redistribution of F-actin into distinct, highly fluorescent foci (Figure 2C, middle right) and to a change in growth cone morphology. Interestingly, TI-VAMP also redistributed to these F-actin-rich foci (Figure 2C, middle left, arrows). Treatment with the cytochalasin B solvent dimethyl sulfoxide (DMSO) alone had no effect on F-actin distribution, growth cone morphology, or on the appearance of TI-VAMP in actin-rich structures (Figure 2C, top). Treatment of neurons with la-

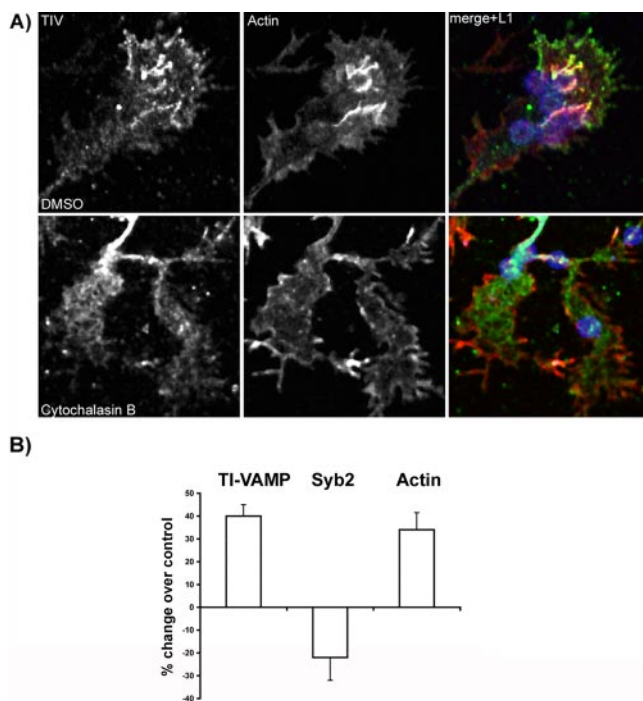


**Figure 3.** Actin-dependent accumulation of TI-VAMP at adhesive contacts. (A) Hippocampal neurons at 3 div were incubated with L1-coated beads in the presence of either DMSO or 5  $\mu$ M cytochalasin B for 45 min. Cells were processed for confocal microscopy with TI-VAMP mAb (green), phalloidin (red), or L1 pAb (blue). Bead-shaped structures can be recognized that are positive for TI-VAMP and F-actin and that coincide with L1-coated beads present on the growth cone shown (merge) (top). Micrographs of cytochalasin B-treated cells show a number of L1-coated beads touching the extremities of the neurite (micrograph L1), but no bead-shaped structures occur that are positive for TI-VAMP or F-actin (bead diameter 4  $\mu$ m). (B) Hippocampal neurons at 3 div were incubated with or without L1-coated beads and stained for TI-VAMP or synaptobrevin 2 and actin. Actin-rich regions of control growth cones or growth cones in contact with beads were selected, and associated fluorescence intensity for TI-VAMP or synaptobrevin 2 and actin was quantified. Shown is the change in intensity for the different markers induced by L1-coated beads compared with control growth cones (TIV: +40.6  $\pm$  5%, n = 41, p = 0.0001; Syb2: -21.7  $\pm$  10%, n = 37, p = 0.037; actin: +34  $\pm$  7.5%, n = 78, p = 0.006).

trunculin A disrupted the actin cytoskeleton more dramatically. Under these conditions, TI-VAMP staining became diffuse, and no accumulation of the protein was observed (Figure 2C, bottom). In contrast, Syb2 did not redistribute to F-actin-rich foci upon treatment with cytochalasin B (Figure 2D, middle) nor did Syb2 staining become diffuse after incubation with latrunculin A (Figure 2D, bottom) compared with its distribution in the control condition (DMSO treatment; Figure 2D, top). Therefore, TI-VAMP accumulation in growth cones depends upon the integrity of the actin cytoskeleton, whereas the localization of Syb2 in growth cones is not obviously affected by actin-sequestering drugs.

The correlated accumulation of F-actin and TI-VAMP in growth cones was observed in neurons grown on poly-L-lysine in a chemically defined medium. Thus, cues leading to an assembly or disassembly of TI-VAMP and F-actin-containing structures cannot be easily deduced. We have previously shown that localized homophilic engagement of the cell adhesion molecule L1 leads to a robust and specific accumulation of TI-VAMP, but not synaptobrevin 2-containing vesicles to sites of contact (Alberts *et al.*, 2003). Furthermore, extensive remodeling of the actin cytoskeleton has been described when growth cones establish contact with a

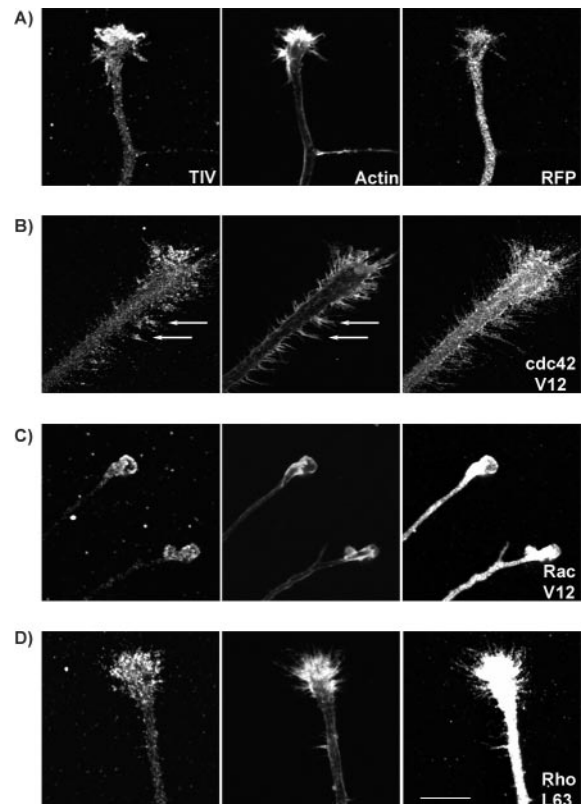


**Figure 4.** Expression of Cdc42V12-RFP induces localization of actin and TI-VAMP to the axonal shaft. Cortical neurons were transfected with RFP (A) or RFP-tagged Cdc42V12 (B), Rac1V12 (C), and RhoAL63 (D) and kept in culture for 5 div at low density. Cells were fixed and stained for TI-VAMP (left), F-actin (middle), and RFP (right). Confocal images of a representative growth cone are shown for each condition. Actin and TI-VAMP do not accumulate at the leading edge of the axon when Cdc42V12 is expressed in cortical neurons. Instead, filopodial structures rich in F-actin and TI-VAMP are seen (arrows). F-actin and TI-VAMP remain in the growth cones of neurons expressing Rac1V12 or RhoAL63. Note the difference in magnification. Bar, 11  $\mu$ m for A, C, and D and 18  $\mu$ m for B.

target cell (Lin and Forscher, 1993). Therefore, we made use of the previously described bead assay to mimic acutely forming L1-dependent contacts in hippocampal neurons (Alberts *et al.*, 2003). The behavior of the TI-VAMP compartment was analyzed with reference to the actin cytoskeleton after incubation of neurons with L1-coated beads. Figure 3A, top, shows that localized ligation of L1 on growth cones leads to a strong accumulation of both TI-VAMP and F-actin to sites of bead–cell contact. We validated these observations by quantifying the fluorescence intensity of TI-VAMP, and, as a control, synaptobrevin 2 associated with actin-rich structures induced by L1-coated beads and compared with actin-rich structures in growth cones not incubated with beads. As shown in Figure 3B, acutely forming L1-dependent contacts induce a local accumulation of both F-actin and TI-VAMP at contact sites compared with control growth cones. In contrast, synaptobrevin 2 seems to be excluded from actin-rich structures forming around L1 beads as the intensity of synaptobrevin 2 staining decreases. Importantly, both the formation of F-actin-rich structures and the accumulation of TI-VAMP by L1-beads were abolished in neurons treated with cytochalasin B (Figure 3A) or latrunculin A (our unpublished observations). Thus, L1-dependent contact formation in growth cones leads to the formation of F-actin-rich structures, which are necessary for the recruitment of the TI-VAMP compartment to sites of bead–growth cone contact.

GTPases of the Rho/Rac/Cdc42 subfamily are of crucial importance in the control of cell polarity and signal-dependent actin remodeling in neurons and other cell types (Luo *et al.*, 1996; Li *et al.*, 2000; Dickson, 2002; Schwamborn and Puschel, 2004; Van Aelst and Cline, 2004). Furthermore, Rac

and Cdc42 were already shown to stimulate exocytosis in mast cells (HongGeller and Cerione, 2000) and Cdc42 regulates exocytosis in adrenal chromaffin cells (Gasman *et al.*, 2004). To investigate whether these GTPases contribute to actin-dependent recruitment of TI-VAMP into growth cones, we expressed dominant-positive (i.e., constitutively active) mutants of RhoA, Rac1, and Cdc42 in cortical neurons. In agreement with previous findings in chick neurons (Brown *et al.*, 2000), we often observed enlarged growth cones and axonal shafts when we expressed dominant-positive Cdc42 mutants in cortical neurons (note the difference in magnification in Figure 4, A and B). A constitutively active Cdc42 mutant, Cdc42V12, expressed as a fusion protein with RFP, localized to the plasma membrane where it induced formation of F-actin-rich filopodia all along the axonal shaft (Figure 4B). In these neurons, TI-VAMP localized to the F-actin-rich filopodia outside the growth cone, accompanied by a large decrease in the intensity of staining for F-actin and TI-VAMP at the leading edge of growing axons (Figure 4B). In control cells, expressing RFP alone (Figure 4A), actin and TI-VAMP remained heavily enriched in the growth cones, as in untransfected neurons (Figures 1 and 2). Despite morphological effects on the growth cones, neither the constitutively active form of Rac (RacV12) or RhoA (RhoL63), expressed as RFP fusion proteins, induced F-actin-rich filopodia outside the growth cone (Figure 4, C and D), and both TI-VAMP and F-actin accumulated normally in the growth cones of cortical neurons expressing either of these mutant proteins.

To evaluate further the role of Cdc42-dependent signaling in this process, we expressed Cdc42V12-RFP and the dominant-negative Cdc42N17-RFP mutant in neurons and stained for actin and TI-VAMP or actin and Syb2. Analysis

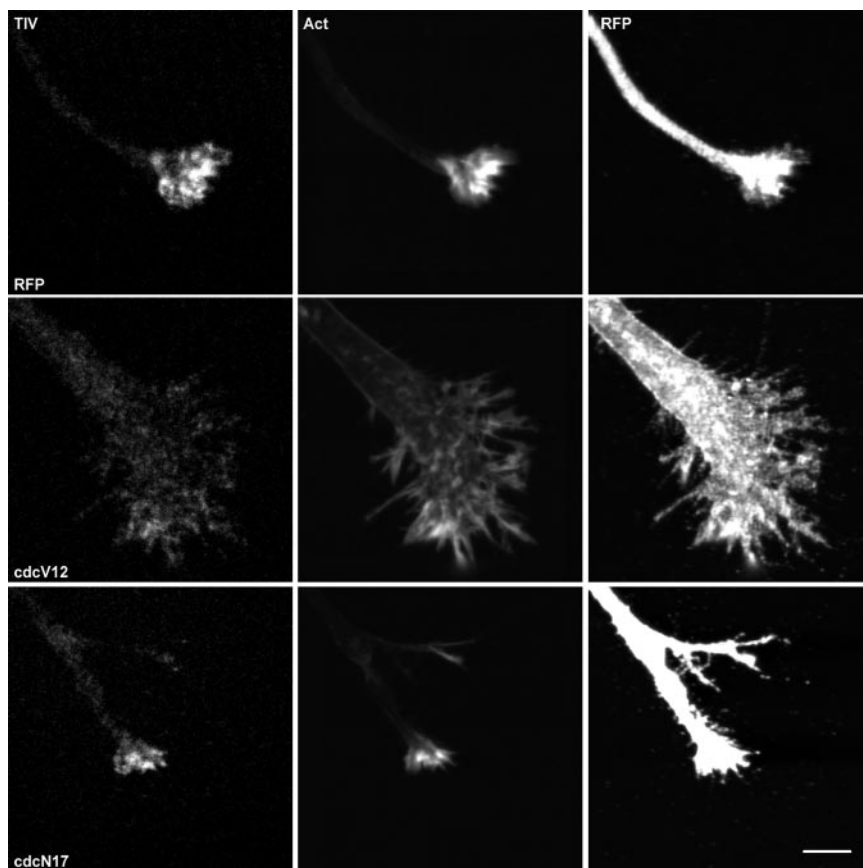


**Figure 5.** Expression of Cdc42V12-RFP and Cdc42N17-RFP interferes with accumulation of TI-VAMP in growth cones. Cortical neurons were transfected with RFP; an RFP-tagged dominant-positive form of Cdc42, Cdc42V12-RFP; or an RFP-tagged dominant-negative form, Cdc42N17-RFP, and kept in culture for 5 d at low density. Cells were fixed and stained for TI-VAMP (left) or F-actin (middle). Confocal images for each condition of a representative growth cone are shown. RFP fluorescence is shown in the right-hand panels. Actin and TI-VAMP do not accumulate at the leading edge of the axon when Cdc42V12-RFP is expressed in cortical neurons and enrichment is reduced by expression of Cdc42N17-RFP. Note the enlarged axonal shaft and growth cone in neurons expressing Cdc42V12-RFP. Bar, 5  $\mu$ m.

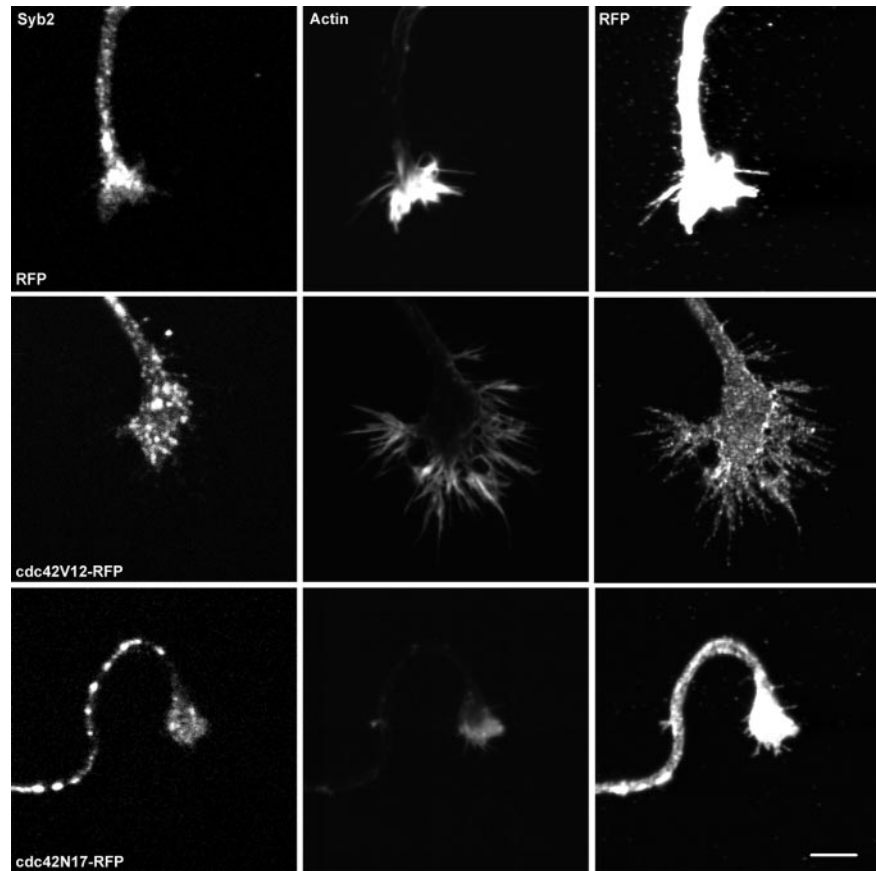


**Figure 6.** Expression of Cdc42V12-RFP and Cdc42N17-RFP does not affect Syb2 localization. Cortical neurons were transfected and processed as described for Figure 4 and stained for Syb2, F-actin, and RFP. Syb2 does not redistribute to the F-actin-rich structures induced by dominant-positive Cdc42V12-RFP but has a similar location in the central domain of growth cones under the three conditions tested. Bar, 5  $\mu$ m.

by confocal microscopy revealed that both dominant-positive and dominant-negative forms of Cdc42 reduced the apparent concentration of TI-VAMP and F-actin in growth cones (Figure 5), whereas Syb2's distribution was not obviously altered by either Cdc42 variant compared with neurons expressing RFP alone (Figure 6). We quantified these observations by measuring the TI-VAMP- or Syb2-associated fluorescence intensity in the F-actin-rich region of the growth cone (Table 1). Dominant-positive Cdc42V12-RFP reduced the mean fluorescence intensity of staining for TI-VAMP and actin in growth cones by  $\approx 50\%$  compared with RFP alone, whereas dominant-negative Cdc42N17-RFP interfered with the accumulation of these proteins to a lesser, although significant extent. The intensity of staining for Syb2 in actin-rich domains of growth cones was low under all conditions tested, and no statistically significant differences were detected compared with cells expressing RFP alone. Therefore, expression of dominant positive or dominant negative Cdc42 in developing neurons strongly affects TI-

VAMP localization and induces a loss of polarized expression of both TI-VAMP and actin in growth cones. In contrast, localization of Syb2 positive organelles seems to be excluded from actin-rich structures in the developing neuron under all conditions tested.

We next established an assay to directly quantify TI-VAMP-dependent exocytosis and evaluate the involvement of the actin cytoskeleton and Rho GTPases in this process. To this end, we generated a pH-sensitive GFP-tagged (Miesenbock *et al.*, 1998; Sankaranarayanan *et al.*, 2000) form of TI-VAMP (TIV-pHL). First, we localized TIV-pHL in Cos7 fibroblastic cells by confocal microscopy and found that its subcellular distribution was identical to the endogenous protein with a high degree of colocalization with CD63 as already published (Martinez-Arca *et al.*, 2003a,b) and a low degree of colocalization with early endosomal antigen 1 (EEA1), an early endosomal marker, as already shown (Coco *et al.*, 1999) (Figure 7A). We were able to show that, as in the case of synapto-pHL, the signal emitted by plasma mem-

**Table 1.** Mean fluorescent intensities in actin-rich domains of growth cones expressing RFP, Cdc42V12-RFP, or Cdc42N17-RFP

	RFP	Cdc42V12	Cdc42N17
TI-VAMP	112.5 $\pm$ 13.1 (n = 19)	55.2 $\pm$ 11.5 (n = 22), p < 0.0001	77.0 $\pm$ 10.4 (n = 21), p = 0.03
Syb2	37.3 $\pm$ 6.3 (n = 15)	28.6 $\pm$ 5.8 (n = 13), p = 0.2099	49.8 $\pm$ 15.5 (n = 13), p = 0.2002
Actin	120.6 $\pm$ 6.8 (n = 30)	78.3 $\pm$ 8.0 (n = 30), p = 0.0005	97.6 $\pm$ 5.6 (n = 29), p = 0.012

Mean values  $\pm$  SE (arbitrary units) of two independent experiments (n = number of neurons). p values were calculated with the Mann-Whitney nonparametric test compared with the RFP data.

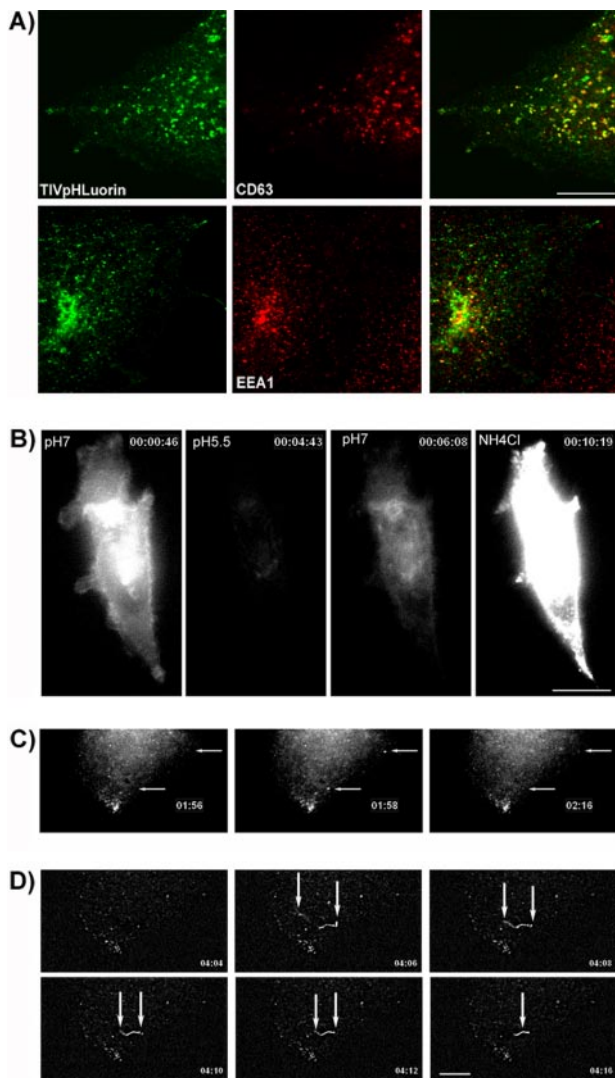


**Figure 7.** Exocytosis of TI-VAMP-containing vesicles in Cos7 cells using TIV-pHL. (A) Cos7 cells were transfected with cDNA encoding TIV-pHL and then fixed and labeled with a polyclonal antibody to GFP (green channel) and with a mAb to CD63, a marker for late endosomes that colocalizes with endogenous TI-VAMP, to EEA1, a marker for early endosomes. Single confocal planes are shown demonstrating a high degree of colocalization between CD63 and TIVpHL (top and bottom, bar, 10  $\mu$ m). (B) Live cell imaging of a Cos7 cell transfected with TIV-pHL in DMEM at pH 7.0. The medium was replaced manually with a saline solution buffered to pH 5.5, changed again with saline solution buffered to pH 7.0, and then treated with 50 mM  $\text{NH}_4\text{Cl}$  in the same buffer (recordings at each condition for 2 min). The epifluorescence signal emitted dropped at pH 5.0 in a reversible manner, indicating that the signal is emitted from TIVpHL present at the cell surface, and the treatment with  $\text{NH}_4\text{Cl}$  resulted in a strong increase of fluorescence because of the contribution from TIVpHL present in intracellular organelles. Bar, 15  $\mu$ m. (C) Cos7 cells were transfected with TIV-pHL and prepared for live imaging. Images were taken every 2 s for 9 min. The images show two exocytic events just before exocytosis (01:56), an exocytotic event as two bright spots (1:58), and after exocytosis and endocytosis/reacidification and disappearance of the TIVpHL signal (2:16) (site of exocytosis is marked by two arrows). (D) Sequence of micrographs of the same cell recorded in A demonstrating the first appearance (4:06) and complete fusion (4:16) of a tubule with the plasma membrane. The right arrow indicates the first point of fusion with the plasma membrane (highest fluorescence intensity at time of appearance), whereas the left arrow points at the intracellular end of the tubule (C and D). Bar, 10  $\mu$ m.

brane resident TIV-pHL as measured by epifluorescence drops reversibly when living cells are incubated at pH 5 and that neutralization of intraorganelle pH with  $\text{NH}_4\text{Cl}$  results in a strong increase of signal because of the signal from intravesicular TIV-pHL (Figure 7B) (Sankaranarayanan *et al.*, 2000; Sankaranarayanan and Ryan, 2000). These results indicate that TIV-pHL fluorescence is quenched intracellularly because of the acidic pH of endosomal organelles and could therefore be used to selectively visualize surface expression of TIV-pHL. When expressed in Cos7 cells, we observed transient puffs of light by time-lapse live cell microscopy that seem similar to secretory vesicle fusion events visualized using synaptotagmin (Figure 7C and Movie 1) (Miesenböck *et al.*, 1998; Sankaranarayanan and Ryan, 2000). Additionally, “worm-like” events could be observed that are likely to represent the fusion of tubules with the plasma membrane (Figure 7D and Movie 1). As indicated by the arrows in Figure 7D, tubular carriers of considerable size (distance between the two arrows in micrograph 7B “4:06” corresponds to  $\sim 18 \mu\text{m}$ ) could be observed.

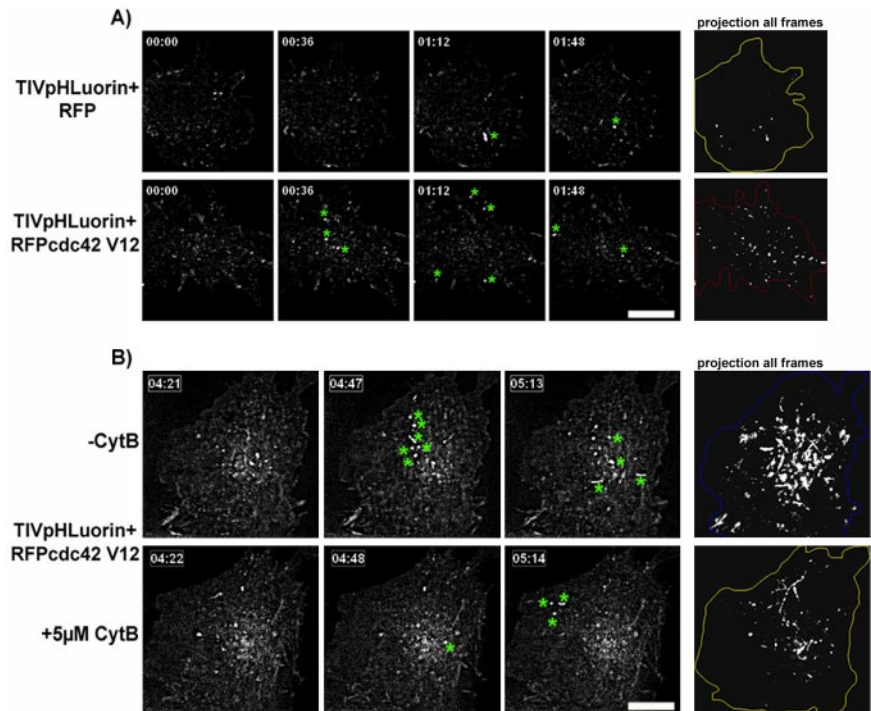
Because dominant-positive Cdc42V12-RFP stimulated the formation of filopodia containing F-actin and TI-VAMP in neurons, we tested the effect of expressing the same construct on the rate of exocytosis of TI-VAMP and compared it with the effect of expressing constitutively active RhoA and Rac1. Unfortunately, expression levels of TIV-pHL were insufficient for detection in neurons and therefore analysis was performed in Cos7 cells. Immunofluorescence analysis showed no obvious differences in localization or expression levels of TIVpHL when RFP or different GTPases were co-expressed (our unpublished data). Cdc42V12-RFP had a very strong stimulatory effect on the exocytosis of TIV-pHL compared with cells expressing RFP alone (see Movie 2 and the corresponding micrographs in Figure 8A). As shown in Table 2, Cdc42V12-RFP increased by  $>10$  the rate of TIV-pHL exocytosis, measured as the number of exocytic events per minute (one representative cell for each condition is presented in Figure 8A). RacV12-RFP had a moderate stimulatory effect (Table 2), whereas RhoL63-RFP was weakly inhibitory (our unpublished data). Importantly, the stimulation by Cdc42V12-RFP depended upon the presence of F-actin because treatment with cytochalasin B strongly inhibited Cdc42V12-RFP-stimulated exocytosis (see Movie 3 and corresponding micrographs in Figure 8B). Thus, enhanced Cdc42 activity stimulates the exocytosis of TI-VAMP in an actin-dependent manner. Taking these data together with those presented in Figure 5, we suggest that the activity of Cdc42, and to a lesser extent, of Rac1 control a pathway linking actin remodeling to the fusion of TI-VAMP-containing vesicles with the plasma membrane.

## DISCUSSION

In contrast to the well-characterized regulatory mechanisms of synaptic vesicle exocytosis in the mature neuron, regulatory mechanisms of membrane trafficking involved in neurite outgrowth are largely unknown. Here, we demonstrate that the dynamic assembly of the actin cytoskeleton and activity of the small GTPase Cdc42 regulates the localization and exocytosis of TI-VAMP.

We found that TI-VAMP but not Syb2 concentrates in neuronal growth cones in an actin-dependent manner, suggesting differential regulation of the compartmentalization of these two vesicular populations in immature neurons. This view is supported by our finding that acute local stimulation of the cell adhesion molecule L1 induces a site-directed accumulation of actin and TI-VAMP, but not syn-

**Figure 8.** Cdc42V12 stimulates F-actin-dependent TIVpHL-mediated exocytosis. (A) Cos7 cells were transfected with TIVpHL together with RFP or Cdc42V12-RFP and analyzed for exocytosis of TIVpHL over 5 min. Stills of representative cells cotransfected with RFP (top) or Cdc42V12-RFP (bottom) are shown. Transient bright TIVpHL spots, representing exocytosis, are marked with green asterisks. Bar, 10  $\mu$ m. Cumulative plots representing the total number of exocytic events during the 5-min recording time for each condition are shown on the right of each series of micrographs, the cell shapes are outlined. (B) Cos7 cells cotransfected as in A were analyzed before and 15 min after treatment with 5  $\mu$ M cytochalasin B. Exocytic events occurring during the sequence shown are marked with asterisks as in A. Bar, 17  $\mu$ m. Corresponding cumulative plots representing the total exocytic events that occurred during the recording time (6.26 min) in each condition are shown on the right of each panel; the shape of the cell recorded before and during CytB treatment is outlined in each case.



aptobrevin 2 (Figure 3; Alberts *et al.*, 2003). It was recently shown that the movements of GFP-Syb2 in growth cones are affected by nocodazole but not cytochalasin B (Sabo and McAllister, 2003), thus pointing to the fact that the dynamics of Syb2 depend more on microtubules than on actin. We also tested the effect of nocodazole and taxol and did not find any significant difference in the polarized concentration of TI-VAMP in growth cones (our unpublished observations). The present article and the study by Sabo *et al.*, (2003) therefore suggest that actin and tubulin play different functions in the compartmentalization of TI-VAMP and Syb2 in the growth cone. A likely explanation of our findings would be that F-actin targets and/or restrains the TI-VAMP, but not the Syb2, vesicles into the growth cone. Syb2 containing organelles may only be transported to the leading edge when a synapse is being generated or stabilized, as suggested by the redistribution of Syb2 to the leading edge of growth cones activated by presynaptic AMPA receptors (Schenk *et al.*, 2003).

We do not know whether the TI-VAMP vesicles are mobile within the actin-rich growth cones or whether they are

sequestered, thus constituting a reserve pool similar to synaptic vesicles in the mature synapse, which are tethered to an actin scaffold by synapsins and are mobilized by a phosphorylation-dependent mechanism (Sudhof, 2004). Our data indicate that TI-VAMP vesicles are directly linked to actin and rapidly mobilized to sites of growth upon signal-induced actin remodeling. TI-VAMP redistributes to actin foci after treatment with cytochalasin B or expression of Cdc42 V12 and is recruited to actin-rich structures forming around L1-coated beads. Moreover, actin might play a direct role in the motility and exocytosis of TI-VAMP-containing vesicles toward the plasma membrane because we find TI-VAMP associated with the plasma membrane in actin-rich growth cones (Figure 1) and detect an actin-dependent exocytosis in Cos 7 cells expressing Cdc42 V12 (Figure 8). A role for actin in the movement of endosomes during stimulus-induced transit to the membrane has been shown recently in fibroblasts (Sandilands *et al.*, 2004). Our current working model would predict that actin dynamics control the localization and possibly exocytosis of the TI-VAMP compartment at the leading edge of growth cones and that this process provides an amplification of directed growth by polarized exocytosis.

The variability in actin and TI-VAMP expression in different growth cones suggests that signaling mechanisms exist that lead to the correlated accumulation of both markers. Indeed, Cdc42 activity might represent such a signaling mechanism, because both dominant-positive as well as dominant-negative Cdc42, but not Rho or Rac, interfere with the polarized expression of both actin and TI-VAMP. In comparison with Cdc42V12-RFP, the less dramatic effect of Cdc42N17-RFP, particularly on actin expression in growth cones, may indicate that Cdc42-independent signaling pathways are involved in the control of TI-VAMP and/or actin accumulation in growth cones. Alternatively, expression levels of the constructs might not have been sufficient to completely abrogate Cdc42-dependent signaling.

At this point, it is unclear whether growth cones rich in actin and TI-VAMP represent fast-growing axons. Indeed,

**Table 2.** Exocytotic activity of Cos 7 cells coexpressing TIVpHL and RFP, Rac1 V12, or Cdc42 V12

	No. of cells analyzed/condition	Exocytotic active cells/total cell no. (%)	No. of exocytotic events/min
RFP	15	13	1.15 $\pm$ 0.2
Rac1 V12	15	27	3.15 $\pm$ 1.9
Cdc42 V12	15	60	17 $\pm$ 2.6

Exocytotic active cells represent the percentage of cells per condition showing recognizable exocytotic activity. Out of those cells, the mean number of exocytotic events per minute for each condition was determined.



we used concentrations of actin-depolymerizing drugs that were previously shown to have no effect on axonal outgrowth in hippocampal neurons (Rajnicsek and McCaig, 1997; Bradke and Dotti, 1999; Dent and Kalil, 2001) but that were shown to abrogate attraction or repulsion of growth cones by guidance cues (Zheng *et al.*, 1996; Rajnicsek and McCaig, 1997). Thus, the accumulation of the TI-VAMP-positive membrane compartment might not be necessary for efficient neurite outgrowth. Rather, it can be speculated that the actin-dependent accumulation of the TI-VAMP compartment in the growth cone periphery may represent a mechanism to integrate actin- and membrane-dynamics to support directed growth. In this light, our finding that Cdc42 and the cell adhesion molecule L1, both of which play important roles in axonal pathfinding (Cohen *et al.*, 1998; Yuan *et al.*, 2003) can coordinate the localization of both actin and TI-VAMP in neuronal growth cones is particularly intriguing.

We did not find any Cdc42 effectors in the several yeast two-hybrid screens that we have carried out in fly embryo, human placenta (Martinez-Arca *et al.*, 2003b; Formstecher *et al.*, 2005), and human fetal brain (our unpublished observations) libraries using the Longin domain or the full cytoplasmic domain of TI-VAMP as baits. Furthermore, the recombinant cytosolic domain of TI-VAMP did not affect directly actin dynamics in vitro (Carlier and Thierry, unpublished observations). Therefore, the details of the molecular mechanism linking Cdc42 activation, TI-VAMP, and actin are likely to involve a complex network that will require further investigations.

In conclusion, our results are consistent with a model in which the restricted activity of Cdc42 within the growth cone mediates the polarized accumulation and exocytosis of TI-VAMP in growth cones through its regulatory action on the actin cytoskeleton. The importance of spatially restricted Cdc42 activation for directed cellular movement was demonstrated before as both dominant-positive and dominant-negative Cdc42 mutants inhibit cellular polarization and directed migration of macrophages and astrocytes (Allen *et al.*, 1998; Etienne-Manneville and Hall, 2001). We do not know the molecular cascade leading to the concentration of TI-VAMP in the growth cone and the stimulation of its exocytosis by Cdc42 in a physiological context. Yet local activation of the cell adhesion molecule L1 in neuronal growth cones induces an actin-dependent recruitment of TI-VAMP-, but not Syb2-containing vesicles, to sites of contact (Figure 3; Alberts *et al.*, 2003). Thus, it seems likely that signaling events induced by adhesion molecules like L1 activate Cdc42 leading to the actin dependent accumulation and exocytosis of TI-VAMP. The mechanism proposed here is similar to that described for phagocytosis in macrophages, another cellular process that also requires localized TI-VAMP trafficking (Braun *et al.*, 2004) upon receptor and Cdc42 activation (Hoppe and Swanson, 2004) and actin remodeling (May and Machesky, 2001). Thus, it is tempting to speculate that TI-VAMP-mediated exocytosis and actin dynamics are tightly coupled to direct the formation of cell protrusions not only in neurons and macrophages but also in other cell types, as a more general mechanism for the formation of directed cellular extensions.

## ACKNOWLEDGMENTS

We are grateful to Julien Cau for the mRFP-Rho GTPases constructs. This work was supported in part by grants from Institut National de la Santé et de la Recherche Médicale (Avenir Program), the European Commission ("Signaling and Traffic" STREP 503229), the Association pour la Recherche sur le

Cancer, the Association Française contre les Myopathies, the Ministère de la Recherche (Action Concertée Incitative-Biologie du Développement et Physiologie Intégrative), the Fondation pour la Recherche Médicale, the Human Frontier Science Program (RGY0027/2001-B101), and the Fondation pour la Recherche sur le Cerveau.

## REFERENCES

- Alberts, P., *et al.* (2003). Cross talk between tetanus neurotoxin-insensitive vesicle-associated membrane protein-mediated transport and L1-mediated adhesion. *Mol. Biol. Cell* 14, 4207–4220.
- Allen, W. E., Zicha, D., Ridley, A. J., and Jones, G. E. (1998). A role for Cdc42 in macrophage chemotaxis. *J. Cell Biol.* 141, 1147–1157.
- Bradke, F., and Dotti, C. G. (1999). The role of local actin instability in axon formation. *Science* 283, 1931–1934.
- Braun, V., Fraissier, V., Raposo, G., Hurbain, I., Sibarita, J. B., Chavrier, P., Galli, T., and Niedergang, F. (2004). TI-VAMP/VAMP7 is required for optimal phagocytosis of opsonised particles in macrophages. *EMBO J.* 23, 4166–4176.
- Brown, M. D., Cornejo, B. J., Kuhn, T. B., and Bamberg, J. R. (2000). Cdc42 stimulates neurite outgrowth and formation of growth cone filopodia and lamellipodia. *J. Neurobiol.* 43, 352–364.
- Chang, S., and De Camilli, P. (2001). Glutamate regulates actin-based motility in axonal filopodia. *Nat. Neurosci.* 4, 787–793.
- Coco, S., Raposo, G., Martinez, S., Fontaine, J. J., Takamori, S., Zahraoui, A., Jahn, R., Matteoli, M., Louvard, D., and Galli, T. (1999). Subcellular localization of tetanus neurotoxin-insensitive vesicle-associated membrane protein (VAMP)/VAMP7 in neuronal cells: evidence for a novel membrane compartment. *J. Neurosci.* 19, 9803–9812.
- Cohen, N. R., Taylor, J. S., Scott, L. B., Guillery, R. W., Soriano, P., and Furley, A. J. (1998). Errors in corticospinal axon guidance in mice lacking the neural cell adhesion molecule L1. *Curr. Biol.* 8, 26–33.
- da Silva, J. S., and Dotti, C. G. (2002). Breaking the neuronal sphere: regulation of the actin cytoskeleton in neurogenesis. *Nat. Rev. Neurosci.* 3, 694–704.
- Dent, E. W., and Kalil, K. (2001). Axon branching requires interactions between dynamic microtubules and actin filaments. *J. Neurosci.* 21, 9757–9769.
- Dickson, B. J. (2002). Molecular mechanisms of axon guidance. *Science* 298, 1959–1964.
- Etienne-Manneville, S., and Hall, A. (2001). Integrin-mediated activation of Cdc42 controls cell polarity in migrating astrocytes through PKCzeta. *Cell* 106, 489–498.
- Filippini, F., Rossi, V., Galli, T., Budillon, A., D'Urso, M., and D'Esposito, M. (2001). Longins: a new evolutionary conserved VAMP family sharing a novel SNARE domain. *Trends Biochem. Sci.* 26, 407–409.
- Formstecher, E., *et al.* (2005). Protein interaction mapping: a *Drosophila* case study. *Genome Res.* 15, 376–384.
- Gasman, S., Chasserot-Golaz, S., Malacombe, M., Way, M., and Bader, M. F. (2004). Regulated exocytosis in neuroendocrine cells: a role for subplasmalemmal Cdc42/N-WASP-induced actin filaments. *Mol. Biol. Cell* 15, 520–531.
- Gauthier-Rouviere, C., Vignal, E., Meriane, M., Roux, P., Montcourier, P., and Fort, P. (1998). RhoG GTPase controls a pathway that independently activates Rac1 and Cdc42Hs. *Mol. Biol. Cell* 9, 1379–1394.
- Grosse, G., Grosse, J., Tapp, R., Kuchinke, J., Gorsleben, M., Fetter, I., Hohne-Zell, B., Gratzl, M., and Bergmann, M. (1999). SNAP-25 requirement for dendritic growth of hippocampal neurons. *J. Neurosci. Res.* 56, 539–546.
- Guirland, C., Suzuki, S., Kojima, M., Lu, B., and Zheng, J. Q. (2004). Lipid rafts mediate chemotropic guidance of nerve growth cones. *Neuron* 42, 51–62.
- HongGeller, E., and Cerione, R. A. (2000). Cdc42 and Rac stimulate exocytosis of secretory granules by activating the IP3/calcium pathway in RBL-2H3 mast cells. *J. Cell Biol.* 148, 481–493.
- Hoppe, A. D., and Swanson, J. A. (2004). Cdc42, Rac1, and Rac2 display distinct patterns of activation during phagocytosis. *Mol. Biol. Cell* 15, 3509–3519.
- Li, Z., Van Aelst, L., and Cline, H. T. (2000). Rho GTPases regulate distinct aspects of dendritic arbor growth in *Xenopus* central neurons in vivo. *Nat. Neurosci.* 3, 217–225.
- Lin, C. H., and Forscher, P. (1993). Cytoskeletal remodeling during growth cone-target interactions. *J. Cell Biol.* 121, 1369–1383.
- Luo, L., Hensch, T. K., Ackerman, L., Barbel, S., Jan, L. Y., and Jan, Y. N. (1996). Differential effects of the Rac GTPase on Purkinje cell axons and dendritic trunks and spines. *Nature* 379, 837–840.

- Martinez-Arca, S., Alberts, P., Zahraoui, A., Louvard, D., and Galli, T. (2000). Role of tetanus neurotoxin insensitive vesicle-associated membrane protein (TI-VAMP) in vesicular transport mediating neurite outgrowth. *J. Cell Biol.* *149*, 889–899.
- Martinez-Arca, S., Coco, S., Mainguy, G., Schenk, U., Alberts, P., Bouille, P., Mezzina, M., Prochiantz, A., Matteoli, M., Louvard, D., and Galli, T. (2001). A common exocytic mechanism mediates axonal and dendritic outgrowth. *J. Neurosci.* *21*, 3830–3838.
- Martinez-Arca, S., Proux-Gillardeaux, V., Alberts, P., Louvard, D., and Galli, T. (2003a). Ectopic expression of syntaxin 1 in the ER redirects TI-VAMP- and cellubrevin-containing vesicles. *J. Cell Sci.* *116*, 2805–2816.
- Martinez-Arca, S., *et al.* (2003b). A dual mechanism controlling the localization and function of exocytic v-SNAREs. *Proc. Natl. Acad. Sci. USA* *100*, 9011–9016.
- May, R. C., and Machesky, L. M. (2001). Phagocytosis and the actin cytoskeleton. *J. Cell Sci.* *114*, 1061–1077.
- Miesenbock, G., DeAngelis, D. A., and Rothman, J. E. (1998). Visualizing secretion and synaptic transmission with pH-sensitive green fluorescent proteins. *Nature* *394*, 192–195.
- Murthy, M., Garza, D., Scheller, R. H., and Schwarz, T. L. (2003). Mutations in the exocyst component Sec5 disrupt neuronal membrane traffic, but neurotransmitter release persists. *Neuron* *37*, 433–447.
- Muzerelle, A., Alberts, P., Martinez-Arca, S., Jeannequin, O., Lafaye, P., Mazie, J.-C., Galli, T., and Gaspar, P. (2003). Tetanus neurotoxin-insensitive vesicle-associated membrane protein localizes to a presynaptic membrane compartment in selected terminal subsets of the rat brain. *Neuroscience* *122*, 59–75.
- Osen-Sand, A., Staple, J. K., Naldi, E., Schiavo, G., Rossetto, O., Petitpierre, S., Malgaroli, A., Montecucco, C., and Catsicas, S. (1996). Common and distinct fusion proteins in axonal growth and transmitter release. *J. Comp. Neurol.* *367*, 222–234.
- Rajnicek, A., and McCaig, C. (1997). Guidance of CNS growth cones by substratum grooves and ridges: effects of inhibitors of the cytoskeleton, calcium channels and signal transduction pathways. *J. Cell Sci.* *110*, 2915–2924.
- Rossi, V., Banfield, D. K., Vacca, M., Dietrich, L. E., Ungermann, C., D'Esposito, M., Galli, T., and Filippini, F. (2004). Longins and their longin domains: regulated SNAREs and multifunctional SNARE regulators. *Trends Biochem. Sci.* *29*, 682–688.
- Rothman, J. E. (2002). The machinery and principles of vesicle transport in the cell. *Nat. Med.* *8*, 1059–1062.
- Sabo, S. L., and McAllister, A. K. (2003). Mobility and cycling of synaptic protein-containing vesicles in axonal growth cone filopodia. *Nat. Neurosci.* *6*, 1264–1269.
- Sandilands, E., Cans, C., Fincham, V. J., Brunton, V. G., Mellor, H., Prendergast, G. C., Norman, J. C., Superti-Furga, G., and Frame, M. C. (2004). RhoB and actin polymerization coordinate Src activation with endosome-mediated delivery to the membrane. *Dev. Cell* *7*, 855–869.
- Sankaranarayanan, S., DeAngelis, D., Rothman, J. E., and Ryan, T. A. (2000). The use of pHluorins for optical measurements of presynaptic activity. *Biophys. J.* *79*, 2199–2208.
- Sankaranarayanan, S., and Ryan, T. A. (2000). Real-time measurements of vesicle-SNARE recycling in synapses of the central nervous system. *Nat. Cell Biol.* *2*, 197–204.
- Schenk, U., Verderio, C., Benfenati, F., and Matteoli, M. (2003). Regulated delivery of AMPA receptor subunits to the presynaptic membrane. *EMBO J.* *22*, 558–568.
- Schoch, S., Deak, F., Konigstorfer, A., Mozhayeva, M., Sara, Y., Sudhof, T. C., and Kavalali, E. T. (2001). SNARE function analyzed in synaptobrevin/VAMP knockout mice. *Science* *294*, 1117–1122.
- Schwamborn, J. C., and Puschel, A. W. (2004). The sequential activity of the GTPases Rap1B and Cdc42 determines neuronal polarity. *Nat. Neurosci.* *7*, 923–929.
- Song, H., and Poo, M. (2001). The cell biology of neuronal navigation. *Nat. Cell Biol.* *3*, E81–88.
- Sudhof, T. C. (2004). The synaptic vesicle cycle. *Annu. Rev. Neurosci.* *27*, 509–547.
- Suter, D. M., Errante, L. D., Belotserkovsky, V., and Forscher, P. (1998). The immunoglobulin superfamily cell adhesion molecule, apCAM, mediates growth cone steering by substrate-cytoskeletal coupling. *J. Cell Biol.* *141*, 227–240.
- Van Aelst, L., and Cline, H. T. (2004). Rho GTPases and activity-dependent dendrite development. *Curr. Opin. Neurobiol.* *14*, 297–304.
- Yuan, X. B., Jin, M., Xu, X., Song, Y. Q., Wu, C. P., Poo, M. M., and Duan, S. (2003). Signalling and crosstalk of Rho GTPases in mediating axon guidance. *Nat. Cell Biol.* *5*, 38–45.
- Zheng, J. Q., Wan, J. J., and Poo, M. M. (1996). Essential role of filopodia in chemotropic turning of nerve growth cone induced by a glutamate gradient. *J. Neurosci.* *16*, 1140–1149.